CHIRAL CONDENSATE
AND CHEMICAL FREEZE-OUT

D. B. Blaschke [a,b,1], *J. Berdermann* [c], *J. Cleymans* [d], *K. Redlich* [a,e]

[a] Institute for Theoretical Physics, University of Wroclaw, Wroclaw, Poland

[b] Joint Institute for Nuclear Research, Dubna

[c] DESY Zeuthen, Zeuthen, Germany

[d] UCT-CERN Research Centre and Department of Physics, Cape Town, South Africa

[e] ExtreMe Matter Institute EMMI, GSI, Darmstadt, Germany

We consider a chemical freeze-out mechanism which is based on a strong medium dependence of the rates for inelastic flavor-equilibrating collisions based on the delocalization of hadronic wave functions and growing hadronic radii when approaching the chiral restoration. We investigate the role of mesonic (pion) and baryonic (nucleon) fluctuations for melting the chiral condensate in the phase diagram in the (T, μ)-plane. We apply the PNJL model beyond mean field and present an effective generalization of the chiral perturbation theory result which accounts for the medium dependence of the pion decay constant while preserving the GMOR relation. We demonstrate within a schematic resonance gas model consisting of a variable number of pionic and nucleonic degrees of freedom that within the above model a quantitative explanation of the hadonic freeze-out curve and its phenomenological conditions can be given.

PACS: 12.38.Mh; 25.75.-q; 24.10.Pa

INTRODUCTION

The investigation of the phase diagram of QCD in the plane of temperature T and baryochemical potential μ_B is one of the goals of heavy-ion collision experiments, of lattice QCD (LQCD) and effective field theory approaches to the nonperturbative sector of QCD. Of particular interest are the conditions under which the approximate chiral symmetry of the QCD Lagrangian will get restored and whether this transition will be necessarily accompanied by the deconfinement of quarks and gluons. More detailed questions to the QCD phase diagram concern the order of these phase transitions, their critical exponents and fluctuation measures as well as the possible existence of a critical point or even a triple point in the phase diagram. Most promising tools for the experimental determination of these characteristics are the energy scan programs at CERN, RHIC and at the upcoming dedicated facilities of the third generation: FAIR and NICA. The systematic analysis of higher moments of distributions of produced particles in their dependence on the collision energy and the size of colliding systems shall provide answers to the above questions and allow direct comparison

---

[1] E-mail: blaschke@ift.uni.wroc.pl

with predictions from the underlying theory, as provided by LQCD, see, e.g., [1] and works cited therein.

As long as the applicability of LQCD methods is bound to the region of finite T and $\mu_B/T \ll 1$, any predictions for the phase structure of QCD at high baryon densities including the possible existence of critical points will rely on effective models. To be relevant for the discussion of the above problems, these models have to share with QCD the property of chiral symmetry and its dynamical breaking as well as a mechanism for confinement and deconfinement.

At the present stage, of particular relevance for the discussion of the QCD phase diagram are the chemical freeze-out parameters (T^f, μ_B^f) which have been obtained from the statistical model analysis of particle yields obtained in heavy-ion collisions [2, 3]. One of the most striking observations is the systematic behavior of these parameters with collision energy $\sqrt{s}$ [4–6], which has recently been given a simple parametric form [7]. It has been observed that the resulting freeze-out curve in the phase diagram is closely correlated to the thermodynamical quantities of the hadron resonance gas described by the statistical model. These phenomenological freeze-out conditions make statements about the mean energy per hadron $\langle E \rangle / \langle N \rangle \simeq 1.0$ GeV, the dimensionless entropy density $s/T^3 \simeq$ 7 and a total baryon and antibaryon density $n_B + n_{\bar{B}} \simeq 0.12$ fm^{-3}. The freeze-out line provides a lower bound for the chiral restoration and deconfinement transition in the phase diagram. Being coincident at low densities as inferred from LQCD [8], both transitions need not to occur simultaneously at high density, thus allowing for an island of a quarkyonic phase [9] between hadron gas and quark–gluon plasma with a (pseudo-)triple point [10].

The question appears for the physical mechanism which governs the chemical freeze-out and which determines quantitatively the freeze-out parameters. One aspect is provided by the requirement that hadrons should overlap in order to facilitate flavor exchange reactions which establish chemical equilibrium. This geometrical picture of freeze-out is sucessfully realized in a percolation theory approach [11]. Another aspect is the dynamical one: when the equation of state (EoS) possesses softest points (e.g., due to the dissociation of hadrons into their quark and gluon constituents with a sufficient release of binding energy involved) which is correlated with the freeze-out curve in the phase diagram, it is obvious that the hadron abundances are characterized by the corresponding T and μ_B values [12]. The dynamical system got quasi-trapped at the softest points for sufficient time to achieve chemical equilibration before evaporating as a gas of hadron resonances freely streaming to the particle detectors. Also the kinetic aspect of fast chemical equilibration was discussed in the hadronic gas when accounting for a multi-hadron dynamics [13].

All these mechanisms are appealing since they provide an intuitively clear picture, but they are flawed by the fact that their relation to fundamental aspects of the QCD phase transition like the chiral condensate as an order parameter is not an element of the description.

In the present contribution we develop an approach which relates the geometrical as well as the hydrodynamic and kinetic aspects of chemical freeze-out to the medium dependence of the chiral condensate. We demonstrate within a beyond-mean-field extension [14–20] of the Polyakov NJL model [21–27] how the excitation of hadronic resonances initiates the melting of the chiral condensate which entails a Mott–Anderson type delocalization of the hadron wave functions and a sudden drop in the relaxation time for flavor equilibra-

tion. Already for a schematic resonance gas consisting of pions and nucleons with artificially enhanced numbers of degrees of freedom, we can demonstrate that a kinetic freeze-out condition for the above model provides quantitative agreement with the phenomenological freeze-out curve.

1. CHEMICAL FREEZE-OUT AND CHIRAL CONDENSATE

We propose to relate the chemical freeze-out to the chiral condensate in the following effective way. As a freeze-out condition for flavor equilibrating reaction kinetics in the temperature-chemical potential plane (T, μ) we employ

$$\tau_{\exp}(T, \mu) = \tau_{\text{coll}}(T, \mu), \tag{1}$$

where $\tau_{\exp}(T, \mu)$ is the expansion time scale of the hadronic fireball and the inverse of the relaxation time for reactive collisions is

$$\tau_{\text{coll}}^{-1}(T, \mu) = \sum_{i,j} \sigma_{ij} n_j, \tag{2}$$

with $i, j = \pi, N, \ldots$ running over all species in the hadron resonance gas. For the cross sections we adopt the geometrical Povh–Hüfner law [28, 29]:

$$\sigma_{ij} = \lambda \langle r_i^2 \rangle \langle r_j^2 \rangle, \tag{3}$$

where λ is a constant of the order of the string tension $\lambda \sim 1 \text{ GeV/fm} = 5 \text{ fm}^{-2}$. Note that this behavior has been obtained for the quark exchange contribution to hadron–hadron cross sections [30].

A key point of our approach is that the radii of hadrons will depend on T and μ and will diverge when hadron dissociation (Mott effect) sets in, driven basically by the restoration of chiral symmetry. This has quantitatively been studied for the pion [31], where it has been shown that close to the Mott transition the chiral perturbation theory corrections can be safely neglected and the pion radius is well approximated by

$$r_\pi^2(T, \mu) = \frac{3}{4\pi^2} f_\pi^{-2}(T, \mu). \tag{4}$$

It has been demonstrated that the GMOR relation holds out to the chiral phase transition where pions would merge the continuum of unbound quark matter [32, 33]. Since the current quark mass is T- and μ-independent and the pion mass is «chirally protected», the T-, μ-dependence of the chiral condensate has to be reflected in a similar behavior of the pion decay constant

$$f_\pi^2(T, \mu) = \frac{-m_0 \langle \bar{q} q \rangle_{T, \mu}}{M_\pi^2}. \tag{5}$$

The resulting relationship between pion radius and chiral condensate in the medium reads

$$r_\pi^2(T, \mu) = \frac{3 M_\pi^2}{4\pi^2 m_q} |\langle \bar{q} q \rangle_{T, \mu}|^{-1}. \tag{6}$$

The delocalization of the pion wave function due to the melting of the chiral condensate as expressed in this formula is the most important element of the hadronic freeze-out mechanism suggested in this work.

For the nucleon, we shall assume the radius to consist of two components, a medium-independent hard core radius r_0 and a pion cloud contribution:

$$r_N^2(T, \mu) = r_0^2 + r_\pi^2(T, \mu), \tag{7}$$

where from the vacuum values $r_\pi = 0.59$ fm and $r_N = 0.74$ fm one gets $r_0 = 0.45$ fm.

For the expansion time scale we adopt a relationship which follows from entropy conservation, $S = s(T, \mu) \, V(\tau_{\mathrm{exp}}) = $ const, and a fireball expansion law $V(\tau_{\mathrm{exp}})$. Assuming that $V(\tau_{\mathrm{exp}}) \propto \tau_{\mathrm{exp}}^3$, one obtains

$$\tau_{\mathrm{exp}}(T, \mu) = a \, s^{-1/3}(T, \mu), \tag{8}$$

with a being a constant of the order one.

As a first step, we will restrict the discussion to a medium consisting of pions and nucleons only, whereby we apply the above relationships. The generalization to a hadron resonance gas along these lines is rather straightforward.

In the following we introduce properties of the chiral condensate in a pion–nucleon and in a hadron resonance gas and then applying the freeze-out condition (2) we compare our model results with phenomenological findings on hadronic freeze-out and its conditions.

2. CHIRAL CONDENSATE BEYOND MEAN FIELD

We start from the general definition of the chiral condensate

$$\langle \bar{q}q \rangle = \frac{\partial}{\partial m_0} \Omega(T, \mu). \tag{9}$$

The thermodynamical potential $\Omega(T, \mu)$ can be decomposed into contributions from the quark and gluon mean field, and hadronic (quantized) fluctuations in the meson and baryon channels

$$\Omega(T, \mu) = \Omega_{\mathrm{MF}}(T, \mu) + \Omega_{\mathrm{meson}}(T, \mu) + \Omega_{\mathrm{baryon}}(T, \mu) - \Omega(0, 0). \tag{10}$$

The subtraction of $\Omega(0, 0)$ removes vacuum divergencies and guarantees that the thermodynamical potential, i.e., pressure and energy density, of the vacuum vanish.

The mean-field contribution is given by [36]

$$\Omega_{\mathrm{MF}}(T, \mu) = -2N_f \int \frac{d^3 p}{(2\pi)^3} \Big\{ 3\varepsilon_p + T \ln \Big[1 + 3\Phi \, \mathrm{e}^{-\beta(\varepsilon_p - \mu)} + $$

$$+ 3\Phi \, \mathrm{e}^{-2\beta(\varepsilon_p - \mu)} + \mathrm{e}^{-3\beta(\varepsilon_p - \mu)} \Big] + T \ln \Big[1 + 3\Phi \, \mathrm{e}^{-\beta(\varepsilon_p + \mu)} + $$

$$+ 3\Phi \, \mathrm{e}^{-2\beta(\varepsilon_p + \mu)} + \mathrm{e}^{-3\beta(\varepsilon_p + \mu)} \Big] \Big\} + \frac{\sigma^2}{4G} + \mathcal{U}(\Phi; T), \quad (11)$$

where the quasiparticle energy is $\varepsilon_p = \sqrt{p^2 + m^2(T,\mu)}$, and $m(T,\mu) = m_0 + \sigma(T,\mu)$. In the following we will shorten the notation by dropping the arguments of $m(T,\mu) = m$ and $\sigma(T,\mu) = \sigma$. For the Polyakov-loop potential we take the logarithmic form motivated by the $SU(3)$ Haar measure,

$$\mathcal{U}(\Phi, T) = \left[-\frac{1}{2}\, a(T)\, \Phi^2 + b(T) \ln(1 - 6\Phi^2 + 8\Phi^3 - 3\Phi^4) \right] T^4, \tag{12}$$

with the corresponding definitions of $a(T)$ and $b(T)$ [16]. In [14], a dependence of the T_0 parameter on the number of active flavors and on the chemical potential has been suggested. Here we will use $T_0 = 200$ MeV. The mean-field value of the traced Polyakov loop is then given by $\bar{\Phi} = \bar{\Phi}^* = [1 + 2\,\cos(\bar{\phi}_3/T)]/3$.

The quark mass gap is obtained from the extremum condition $\partial\Omega/\partial\sigma = 0$, equivalent to

$$\frac{\sigma}{2G} = \frac{6}{\pi^2} \int dp\, p^2 \frac{m}{\varepsilon_p} \left[1 - f_\Phi^+ - f_\Phi^- \right], \tag{13}$$

where the PNJL quark distribution functions are given by

$$f_\Phi^\pm = \frac{\Phi[\mathrm{e}^{-\beta(\varepsilon_p-\mu)} + 2\,\mathrm{e}^{-2\beta(\varepsilon_p-\mu)}] + \mathrm{e}^{-3\beta(\varepsilon_p-\mu)}}{1 + 3\Phi\,\mathrm{e}^{-\beta(\varepsilon_p-\mu)} + 3\Phi\,\mathrm{e}^{-2\beta(\varepsilon_p-\mu)} + \mathrm{e}^{-3\beta(\varepsilon_p-\mu)}}. \tag{14}$$

The values of the Polyakov loop Φ in the phase diagram are found from a similar gap equation corresponding to the solution of the extremum condition $\partial\Omega/\partial\Phi = 0$.

The contribution of mesonic fluctuations has been discussed in [34, 35] for the NJL model and in [36, 37] for the PNJL model. Also recently mesonic fluctuations were included in these models within the functional renormalization group approach [38, 39].

In the following we consider only the on-mass-shell meson contributions and neglect the continuum correlations beyond the Mott effect. This is justified because we are actually interested in the hadronic freeze-out occurring in a region of the phase diagram which does not exceed the limits of the hadronic phase. This contribution is given as

$$\Omega_{\mathrm{meson}}(T, \mu) = \sum_{M=\pi,...} d_M \int \frac{d^3 k}{(2\pi)^3} \left\{ \frac{E_M(k)}{2} + T \ln\left[1 - \mathrm{e}^{-\beta E_M(k)} \right] \right\}, \tag{15}$$

where the index M denotes the actual meson with degeneracy factor d_M. We restrict this sum to the lowest meson state, the pion, with $E_\pi(k) = \sqrt{k^2 + M_\pi^2}$.

The contribution of pionic fluctuations to the chiral condensate is obtained from

$$\frac{\partial \Omega_\pi}{\partial m_0} = \langle \bar{q}q \rangle_\pi = -\frac{M_\pi n_{s,\pi}}{2m_0} + \langle \bar{q}q \rangle_\pi^{\mathrm{vac}}, \tag{16}$$

where the GMOR relation has been used to evaluate $\partial E_\pi(k)/\partial m_0 = M_\pi^2/(2m_0 E_\pi(k))$ and the scalar pion density has been defined as

$$n_{s,\pi} = \frac{d_\pi}{2\pi^2} \int\limits_0^\infty dp\, p^2 \frac{M_\pi}{E_\pi(p)} \frac{1}{\mathrm{e}^{\beta E_\pi(p)} - 1}. \tag{17}$$

The last term corresponds to a vacuum contribution which gets eliminated by the vacuum subtraction rule (10) inherent in the definition of the full condensate (9).

The contribution of baryons to the partition function is considered as an ideal Fermi gas:

$$\Omega_{\mathrm{baryon}}(T,\mu) = -\sum_{B=N,\dots} d_B \int \frac{d^3k}{(2\pi)^3} \left\{ \frac{E_B(k)}{2} + \right.$$
$$\left. +T\ln\left[1 + \mathrm{e}^{-\beta(E_B(k)-\mu_B)}\right]\right\} + \mu_B \leftrightarrow -\mu_B. \quad (18)$$

For the discussion of the quark condensate, we will focus here on the nucleonic contribution

$$\frac{\partial \Omega_N}{\partial m_0} = \langle\bar{q}q\rangle_N = -\frac{\sigma_N\, n_{s,N}(T,\mu)}{m_0} + \langle\bar{q}q\rangle_N^{\mathrm{vac}}, \quad (19)$$

where we have used the Feynman–Hellman theorem and introduced the pion–nucleon sigma term, $\sigma_N = m_0(\partial m_N/\partial m_0) = 45$ MeV [40].

The nucleon scalar density is given by

$$n_{s,N}(T,\mu) = \frac{d_N}{2\pi^2} \int_0^\infty dp\, p^2 \frac{m_N}{E_N(p)} \left\{ f_N(T,\mu) + f_N(T,-\mu) \right\}, \quad (20)$$

where $f_N(T,\mu) = \{1 + \exp[(\sqrt{p^2 + m_N^2} - \mu_B)/T]\}^{-1}$ is the nucleon Fermi distribution, $m_N = 939$ MeV is the nucleon mass and $\mu_B = 3\mu$ the baryon chemical potential. The vacuum contribution stemming from the zero-point energy term gets removed by the vacuum subtraction procedure (10).

From the above discussion, the chiral condensate in a $\pi - N$ gas can be obtained as

$$-\langle\bar{q}q\rangle = \frac{\sigma}{2G} - \frac{M_\pi n_{s,\pi}(T)}{2m_0} - \frac{\sigma_N\, n_{s,N}(T,\mu)}{m_0}. \quad (21)$$

Note that using the chiral limit expression for the scalar pion density $n_{s,\pi} = d_\pi M_\pi T^2/12$ and the GMOR relation (5), we may put this result in the form

$$\langle\bar{q}q\rangle = \langle\bar{q}q\rangle_{\mathrm{MF}} \left[1 - \frac{T^2}{8f_\pi^2(T,\mu)} - \frac{\sigma_N n_{s,N}(T,\mu)}{M_\pi^2 f_\pi^2(T,\mu)}\right], \quad (22)$$

which is known from the chiral perturbation theory [41,42], but now with a medium-dependent pion decay constant. Since the modification of the mean-field contribution stemming from the quark excitations is proportional to f_Φ, it is now effectively suppressed by the Polyakov loop, compared to the standard NJL model case.

Numerical results for the condensate in the $T-\mu$ plane are given in Fig. 1, where we display contours of equal condensate and indicate its percentage reduction relative to the vacuum value. We use standard values of the NJL model parametrization, e.g., from [43], with $G\Lambda^2 = 2.31825$, $\Lambda = 602.472$ MeV, $m_0 = 5.27697$ MeV, $m_{s,0} = 150$ MeV, $M_\pi = 140$ MeV, $M_K = 495$ MeV, $f_\pi = 92.4$ MeV and $f_K = 93.6$ MeV.
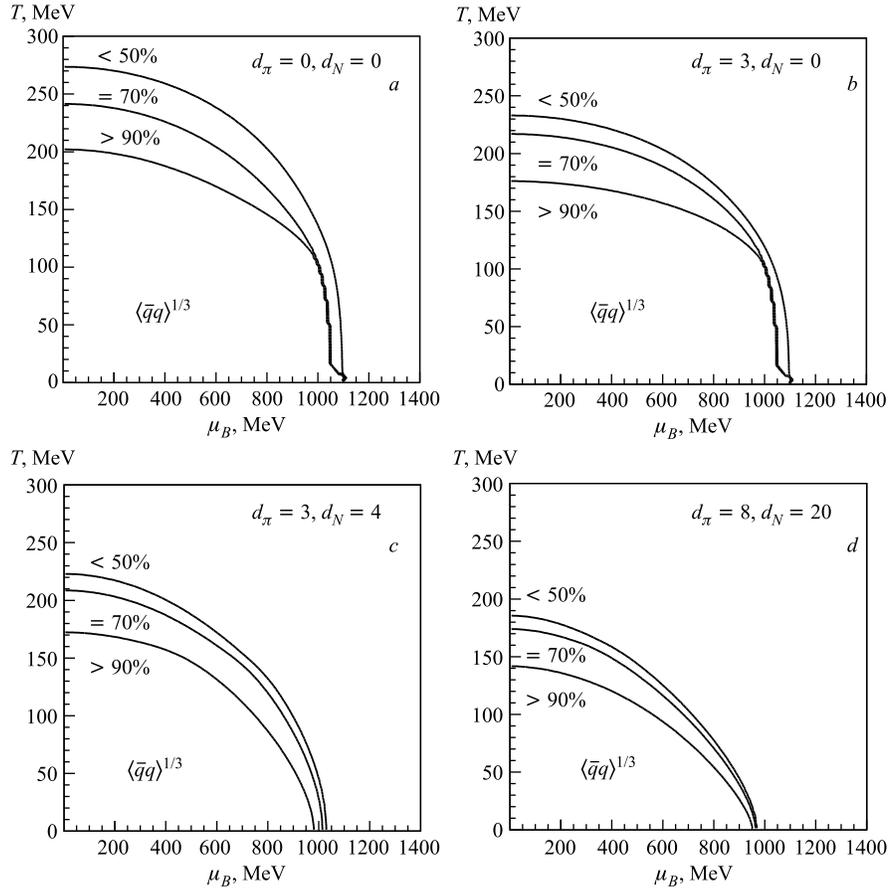
Fig. 1. Behavior of the chiral condensate $\langle q\bar{q} \rangle$ in the PNJL model at mean-field level (*a*), with pion fluctuations (*b*), with pion and nucleon fluctuations (*c*) and for the schematic resonance gas medium with 8 pionic and 20 nucleonic degrees of freedom (*d*). Also shown are the corresponding reductions of the chiral condensate relative to its vacuum value for each set of parameters

3. THE FREEZE-OUT CURVE

In the following we compare predictions of our model on the freeze-out conditions with that obtained within the statistical model analysis of particle yields in heavy-ion collisions.

Figure 2 shows results for different freeze-out curves obtained from the kinetic condition, Eq. (1), applied to the schematic resonance gas model with variable numbers of pion (d_π) and nucleon (d_N) degrees of freedom. The results are compared with the phenomenological values. From this figure, it is clear that for $d_\pi = 8$ and $d_N = 14-20$ there is an excellent correspondence of our freeze-out criterion with phenomenological values. Increasing d_π results in decreasing freeze-out temperatures in the meson-dominated region
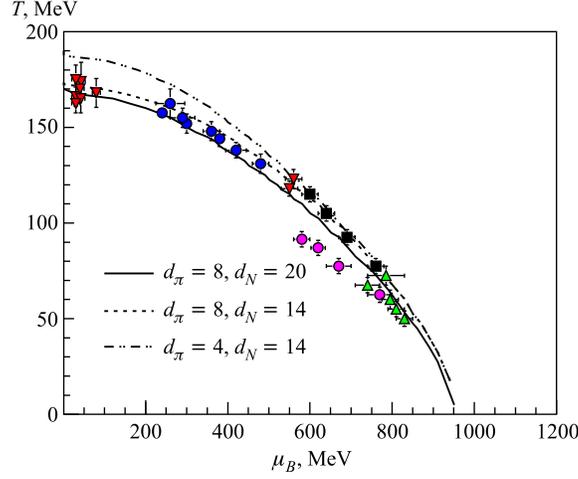
Fig. 2. Freeze-out curves according to the kinetic freeze-out condition, Eq. (1), for the schematic resonance gas model with different number of pion (d_π) and nucleon (d_N) degrees of freedom compared to phenomenological values (symbols) [10]. The lines correspond to different choices for d_π and d_N given in the legend

at small μ_B/T. On the other hand, increasing d_N shifts the entire freeze-out curve towards lower T and μ_B. The freeze-out curves calculated within our model correspond to a reduction of the chiral condensate down to 70 % of its vacuum value, c.f. Fig. 1, d, so that the hadron–hadron cross section in (2) according to (3) is roughly twice the vacuum value.

To verify further our model, we evaluate the entropy density $s(T, \mu) = -\partial\Omega/\partial T$, which according to the statistical model is related to the freeze-out curve by the phenomenological condition, $s(T^f, \mu_B^f)/T^3 \simeq 7$. Figure 3, a shows the comparison of the phenomenological freeze-out points with the lines of constant $s(T, \mu)/T^3$ calculated within our model. The dashed line in this figure corresponds to $s(T, \mu)/T^3 = 7$, which is the freeze-out line obtained within the hadron resonance gas model.

Figure 3, b shows a comparison similar to that in the panel b, but assuming freeze-out conditions of constant density of baryons, $n_B(T^f, \mu_B^f) + \bar{n}_B(T^f, \mu_B^f) = \text{const}$. The nucleon density is obtained from

$$n_N(T, \mu) = \frac{d_N}{2\pi^2} \int\limits_0^\infty k^2 dk \frac{1}{1 + e^{\beta(E_N(k) - \mu_B)}}, \tag{23}$$

where $d_N = 20$ is the number of nucleonic degrees of freedom in our schematic resonance gas and the antinucleon density, $\bar{n}_N(T, \mu) = n_N(T, -\mu)$. The result of the calculation with the above parameters is shown in the panel b of Fig. 3. From this figure one can conclude that our effective model reproduces the phenomenological freeze-out line also when imposing conditions of fixed total density of baryons.
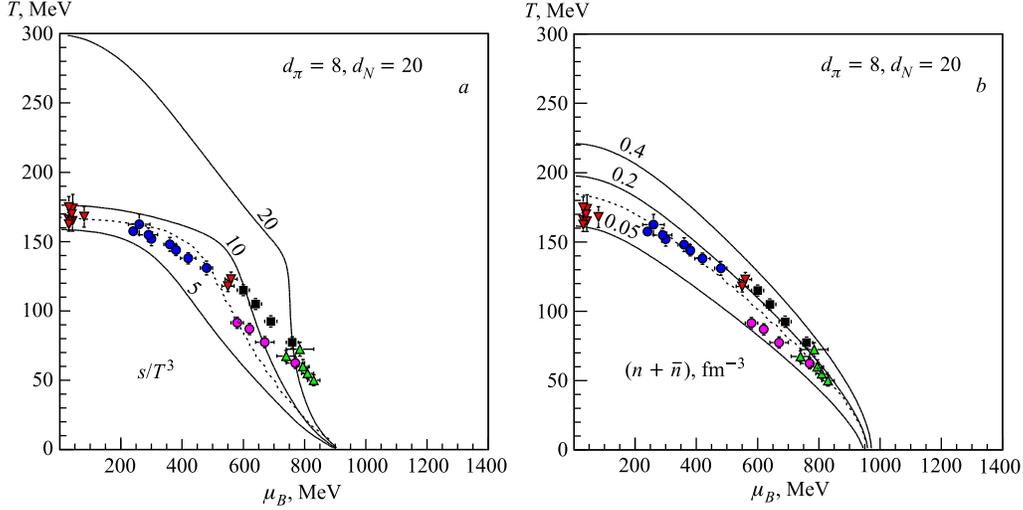
Fig. 3. Entropy s divided by T^3 (a) and total baryon density $n + \bar{n}$ (b) as functions of temperature T and the baryon chemical potential μ_B for the schematic resonance gas model with 8 pion and 20 nucleon degrees of freedom. The dashed curves represent the phenomenological lines of constant: $s(T^f, \mu_B^f)/T^3 = 7$ in plot (a) and $n_B(T^f, \mu_B^f) + \bar{n}_B(T^f, \mu_B^f) = 0.12$ fm^{-3} in plot (b)

4. CONCLUSION AND OUTLOOK

We have developed chemical freeze-out mechanism which is based on a strong medium dependence of the rates for inelastic flavor-equilibrating collisions based on the delocalization of hadronic wave functions and growing hadronic radii when approaching the chiral restoration. This approach relates the geometrical (percolation) as well as the hydrodynamic (softest point) and kinetic (quark exchange) aspects of chemical freeze-out to the medium dependence of the chiral condensate. For our model calculations we have employed a beyond-mean-field *effective* extension of the Polyakov NJL model. We could demonstrate how the excitation of hadronic resonances initiates the melting of the chiral condensate which entails a Mott–Anderson type delocalization of the hadron wavefunctions and a sudden drop in the relaxation time for flavor equilibration. Already for a schematic resonance gas consisting of pions and nucleons with artificially enhanced numbers of degrees of freedom, we could demonstrate that the kinetic freeze-out condition can provide quantitative agreement with the phenomenological freeze-out curve. The further development of this approach would clearly require the replacement of the schematic resonance gas model with the one based on the full spectrum of hadronic resonances and detailed studies of their influence on the chiral condensate. To this end, generalized models for hadron resonance masses are required, which reveal their dependence on the current quark mass like, e.g., the model of Leupold [46]. However, it is very likely that with such extension the model results quantifying freeze-out conditions will still be consistent with phenomenological findings.

REFERENCES

1. *Karsch F., Redlich K.* Probing Freeze-out Conditions in Heavy Ion Collisions with Moments of Charge Fluctuations // Phys. Lett. B. 2011. V. 695. P. 136.

2. *Braun-Munzinger P., Redlich K., Stachel J.* Particle Production in Heavy Ion Collisions. Quark Gluon Plasma 3. World Sci., 2003. P. 491–599; arXiv:nucl-th0304013.

3. *Braun-Munzinger P. et al.* Hadron Production in Au–Au Collisions at RHIC // Phys. Lett. B. 2001. V. 518. P. 41.

4. *Cleymans J., Redlich K.* Unified Description of Freezeout Parameters in Relativistic Heavy Ion Collisions // Phys. Rev. Lett. 1998. V. 81. P. 5284–5286.

5. *Cleymans J., Redlich K.* Chemical and Thermal Freezeout Parameters from 1 A/GeV to 200 A/GeV // Phys. Rev. C. 1999. V. 60. P. 054908.

6. *Cleymans J. et al.* Comparison of Chemical Freeze-out Criteria in Heavy Ion Collisions // Phys. Rev. C. 2006. V. 73. P. 034905.

7. *Cleymans J. et al.* Status of Chemical Freeze-Out // J. Phys. G. 2006. V. 32. P. S165.

8. *Karsch F., Laermann E.* Susceptibilities, the Specific Heat and a Cumulant in Two-Flavor QCD // Phys. Rev. D. 1994. V. 50. P. 6954.

9. *McLerran L., Pisarski R. D.* Phases of Cold, Dense Quarks at Large N_c // Nucl. Phys. A. 2007. V. 796. P. 83.

10. *Andronic A. et al.* Hadron Production in Ultra-relativistic Nuclear Collisions: Quarkyonic Matter and a Triple Point in the Phase Diagram of QCD // Nucl. Phys. A. 2010. V. 837. P. 65–86.

11. *Magas V., Satz H.* Conditions for Confinement and Freeze-Out // Eur. Phys. J. C. 2003. V. 32. P. 115.

12. *Toneev V. D. et al.* Dynamical Interpretation of Chemical Freezeout in Heavy Ion Collisions // J. Phys. G. 2001. V. 27. P. 827–832.

13. *Braun-Munzinger P., Stachel J., Wetterich C.* Chemical Freeze-out and the QCD Phase Transition Temperature // Phys. Lett. B. 2004. V. 596. P. 61.

14. *Schaefer B. J., Pawlowski J. M., Wambach J.* The Phase Structure of the Polyakov–Quark-Meson Model // Phys. Rev. D. 2007. V. 76. P. 074023.

15. *Blaschke D. et al.* Effects of Mesonic Correlations in the QCD Phase Transition // Yad. Fiz. 2008. V. 71. P. 2012.

16. *Roessner S. et al.* The Chiral and Deconfinement Crossover Transitions: PNJL Model beyond Mean Field // Nucl. Phys. A. 2008. V. 814. P. 118.

17. *Blaschke D. et al.* Nonlocal Quark Model beyond Mean Field and QCD Phase Transition // Nucl. Phys. Proc. Suppl. 2010. V. 198. P. 51.

18. *Skokov V. et al.* Meson Fluctuations and Thermodynamics of the Polyakov Loop Extended Quark-Meson Model // Phys. Rev. C. 2010. V. 82. P. 015206.

19. *Skokov V., Friman B., Redlich K.* The Renormalization Group and Quark Number Fluctuations in the Polyakov Loop Extended Quark-Meson Model at Finite Baryon Density. arXiv:1008.4570 [hep-ph].

20. *Radzhabov A. E. et al.* Nonlocal PNJL Model beyond Mean Field and the QCD Phase Transition. arXiv:1012.0664 [hep-ph].

21. *Fukushima K.* Effects of Chiral Restoration on the Behavior of the Polyakov Loop // Prog. Theor. Phys. Suppl. 2003. V. 151. P. 171.

22. *Fukushima K.* Chiral Effective Model with the Polyakov Loop // Phys. Lett. B. 2004. V. 591. P. 277.

23. *Fukushima K.* Relation between the Polyakov Loop and the Chiral Order Parameter at Strong Coupling // Phys. Rev. D. 2003. V. 68. P. 045004.

24. *Fukushima K.* Effects of Chiral Restoration on the Behaviour of the Polyakov Loop at Strong Coupling // Phys. Lett. B. 2003. V. 553. P. 38.

25. *Ratti C., Thaler M. A., Weise W.* Phases of QCD: Lattice Thermodynamics and a Field Theoretical Model // Phys. Rev. D. 2006. V. 73. P. 014019.

26. *Roessner S., Ratti C., Weise W.* Polyakov Loop, Diquarks and the Two-Flavour Phase Diagram // Phys. Rev. D. 2007. V. 75. P. 034007.

27. *Sasaki C., Friman B., Redlich K.* Susceptibilities and the Phase Structure of a Chiral Model with Polyakov Loops // Ibid. P. 074013.

28. *Hüfner J., Povh B.* Diffractive Elastic Scattering and Hadronic Radii: Geometric and Pomeron Approaches // Phys. Rev. D. 1992. V. 46. P. 990.

29. *Povh B., Hüfner J.* Systematics of Strong Interaction Radii for Hadrons // Phys. Lett. B. 1990. V. 245. P. 653.

30. *Martins K., Blaschke D., Quack E.* Quark Exchange Model for Charmonium Dissociation in Hot Hadronic Matter // Phys. Rev. C. 1995. V. 51. P. 2723.

31. *Hippe H. J., Klevansky S. P.* Nambu–Jona-Lasinio Model Compared with Chiral Perturbation Theory: The Pion Radius in $SU(2)$ Revisited // Ibid. V. 52. P. 2172.

32. *Blaschke D., Tandy P. C.* Mesonic Correlations and Quark Deconfinement. Understanding Deconfinement in QCD. World Sci., 2000. P. 218–230; arXiv:9905067 [nucl-th].

33. *Blaschke D. et al.* Finite T Meson Correlations and Quark Deconfinement // Intern. J. Mod. Phys. A. 2001. V. 16. P. 2267.

34. *Zhuang P., Hüfner J., Klevansky S. P.* Thermodynamics of a Quark–Meson Plasma in the Nambu–Jona-Lasinio Model // Nucl. Phys. A. 1994. V. 576. P. 525.

35. *Hüfner J. et al.* Thermodynamics of a Quark Plasma beyond the Mean Field: A Generalized Beth–Uhlenbeck Approach // Ann. Phys. 1994. V. 234. P. 225.

36. *Hansen H. et al.* Mesonic Correlation Functions at Finite Temperature and Density in the Nambu–Jona-Lasinio Model with a Polyakov Loop // Phys. Rev. D. 2007. V. 75. P. 065004.

37. *Hell T. et al.* Dynamics and Thermodynamics of a Non-local PNJL Model with Running Coupling // Phys. Rev. D. 2009. V. 79. P. 014022.

38. *Berges J., Tetradis N., Wetterich C.* // Phys. Rep. 2002. V. 363. P. 223.

39. *Schaefer B. J., Pawlowski J. M., Wambach J.* The Phase Structure of the Polyakov–Quark-Meson Model // Phys. Rev. D. 2007. V. 76. P. 074023;
Stokic B., Friman B., Redlich K. The Functional Renormalization Group and $O(4)$ Scaling // Eur. Phys. J. C. 2010. V. 67. P. 425;
Nakano E. et al. Fluctuations and Isentropes near the Chiral Critical Endpoint // Phys. Lett. B. 2010. V. 682. P. 401;
Skokov V., Friman B., Redlich K. The Renormalization Group and Quark Number Fluctuations in the Polyakov Loop Extended Quark-Meson Model at Finite Baryon Density. arXiv:1008.4570 [hep-ph];
Herbst T. K., Pawlowski J. M., Schaefer B.-J. The Phase Structure of the Polyakov–Quark-Meson Model beyond Mean Field // Phys. Lett. B. 2011. V. 696. P. 58.

40. *Cohen T. D., Furnstahl R. J., Griegel D. K.* Quark and Gluon Condensates in Nuclear Matter // Phys. Rev. C. 1992. V. 45. P. 1881.

41. *Gasser J., Leutwyler H.* Light Quarks at Low Temperatures // Phys. Lett. B. 1987. V. 184. P. 83.

42. *Buballa M.* NJL Model Analysis of Quark Matter at Large Density // Phys. Rep. 2005. V. 407. P. 205.

43. *Grigorian H.* Parametrization of a Nonlocal, Chiral Quark Model in the Instantaneous Three-Flavor Case: Basic Formulas and Tables // Phys. Part. Nucl. Lett. 2007. V. 4. P. 223.

44. *Ebeling W. et al.* Quantum Statistics of Charged Many-Particle Systems. N. Y.: Plenum, 1986.

45. *Blaschke D. et al.* Mott Mechanism and the Hadronic to Quark Matter Phase Transition // Phys. Lett. B. 1985. V. 151. P. 439.

46. *Leupold S.* Four-Quark Condensates and Chiral Symmetry Restoration in a Resonance Gas Model // J. Phys. G. 2006. V. 32. P. 2199–2218.